

Increasing risk of glacial lake outburst floods from future Third Pole deglaciation

Guoxiong Zheng ^{1,2,3,13}, Simon Keith Allen ^{2,4,13}, Anming Bao ^{1,5} , Juan Antonio Ballesteros-Cánovas ^{2,6}, Matthias Huss ^{7,8,9}, Guoqing Zhang ^{10,11}, Junli Li ¹, Ye Yuan ^{1,3}, Liangliang Jiang ^{1,3}, Tao Yu ^{1,3}, Wenfeng Chen ^{3,10} and Markus Stoffel ^{2,6,12}

Warming on Earth's Third Pole is leading to rapid loss of ice and the formation and expansion of glacial lakes, posing a severe threat to downstream communities. Here we provide a holistic assessment of past evolution, present state and modelled future change of glacial lakes and related glacial lake outburst flood (GLOF) risk across the Third Pole. We show that the highest GLOF risk is at present centred in the eastern Himalaya, where the current risk level is at least twice that in adjacent regions. In the future, GLOF risk will potentially almost triple as a consequence of further lake development, and additional hotspots will emerge to the west, including within transboundary regions. With apparent increases in GLOF risk already anticipated by the mid-twenty-first century in some regions, the results highlight the urgent need for forward-looking, collaborative, long-term approaches to mitigate future impacts and enhance sustainable development across the Third Pole.

The Hindu Kush–Himalaya, Tibetan Plateau and surrounding areas are widely known as the Third Pole of the Earth as it is home to the largest number of glaciers outside the polar regions¹. Widespread retreat of glaciers is taking place over most of its territory and has accelerated in recent decades as one of the consequences of global warming^{2–4}. This glacier wasting is associated with the rapid expansion and new formation of glacial lakes^{5–8}, bringing both large opportunities and risks^{9,10}. Particularly, when water is suddenly released, glacial lake outburst floods (GLOFs)¹¹ can devastate lives and livelihoods up to hundreds of kilometres downstream of their source^{12,13}. This threat is most apparent in the Third Pole^{14,15} where the warming rates are distinctly higher than the Northern Hemisphere and global mean¹⁶, and numerous GLOFs have been recorded, originating from both moraine-dammed and ice-dammed glacial lakes^{15,17}. While outbursts from ice-dammed glacial lakes have been concentrated in the Karakoram and Pamir regions^{18,19}, outbursts from moraine-dammed glacial lakes are observed across the Third Pole, and most frequently along the main Himalayan arc²⁰ where glacial lakes are increasing rapidly in both size and number^{5,6}. The impact of a GLOF can extend across international boundaries²¹, creating severe challenges for early warning and other risk reduction strategies, particularly in critical transboundary areas²². Despite the severe threat that such large extreme events pose for sustainable mountain development over the Third Pole⁴, there remains a lack of understanding regarding how and where GLOF risk will evolve in the future. GLOF assessment over the Third Pole has typically been focused on moraine-dammed proglacial lakes owing to their potentially large flood volumes^{23,24}, weak dam composition²⁵ and clear link to climate change¹⁷. Outburst

floods from moraine-dammed glacial lakes can be triggered by various mechanisms, including intense precipitation and snowmelt^{26,27}, and most commonly, from the impact of ice and/or rock avalanches into a lake^{20,28}. While robust long-term trends in GLOF frequency are not evident^{17,29}, the GLOF threat is expected to increase in response to future warming as lakes expand towards steep and destabilizing mountain cliffs^{30,31}. With the expansion of communities, tourism, hydropower, transportation and other crucial sectors into exposed areas, substantial risk reduction and adaptation strategies will be required to avoid increased impacts on sustainable development in vulnerable mountain regions. Focusing here on moraine-dammed proglacial lakes, we draw on a comprehensive inventory of glacial lakes and past GLOF events across the Third Pole, to model and evaluate how and where GLOF hazard and risk will change in response to future deglaciation, using a robust and unified evidence-based approach.

Past evolution and present state of glacial lakes

To understand the present state of glacial lakes across the Third Pole and changes over the past decades, all glacial lakes $\geq 0.01 \text{ km}^2$ were mapped based on archival Landsat satellite images from 1990 to 2015 (Methods). Our inventory reveals the existence of 26,633 glacial lakes in the Third Pole, with a total area of $1,968.8 \pm 1.2 \text{ km}^2$ and approximately one-third of them being dammed by moraines (in total 7,650 with a combined area of $535.1 \pm 0.7 \text{ km}^2$; 6,958 of these lakes were formed in proglacial areas or are in a transitional state). The dataset suggests a clear heterogeneity in their spatial distribution (Fig. 1 and Supplementary Table 1) as today's glacial lakes are principally distributed along the Hindu Kush–Himalaya–Hengduan

¹State Key Laboratory of Desert and Oasis Ecology, Xinjiang Institute of Ecology and Geography, Chinese Academy of Sciences, Urumqi, China. ²Climatic Change Impacts and Risks in the Anthropocene (C-CIA), Institute for Environmental Sciences, University of Geneva, Geneva, Switzerland. ³University of Chinese Academy of Sciences, Beijing, China. ⁴Department of Geography, University of Zurich, Zurich, Switzerland. ⁵China-Pakistan Joint Research Center on Earth Sciences, CAS-HEC, Islamabad, Pakistan. ⁶Dendrolab.ch, Department of Earth Sciences, University of Geneva, Geneva, Switzerland. ⁷Laboratory of Hydraulics, Hydrology and Glaciology (VAW), ETH Zurich, Zurich, Switzerland. ⁸Swiss Federal Institute for Forest Snow and Landscape Research (WSL), Birmensdorf, Switzerland. ⁹Department of Geosciences, University of Fribourg, Fribourg, Switzerland. ¹⁰Institute of Tibetan Plateau Research, Chinese Academy of Sciences, Beijing, China. ¹¹CAS Center for Excellence in Tibetan Plateau Earth Sciences, Beijing, China. ¹²Department of F.A. Forel for Environmental and Aquatic Sciences, University of Geneva, Geneva, Switzerland. ¹³These authors contributed equally: Guoxiong Zheng, Simon Keith Allen. e-mail: baoam@ms.xjb.ac.cn; markus.stoffel@unige.ch

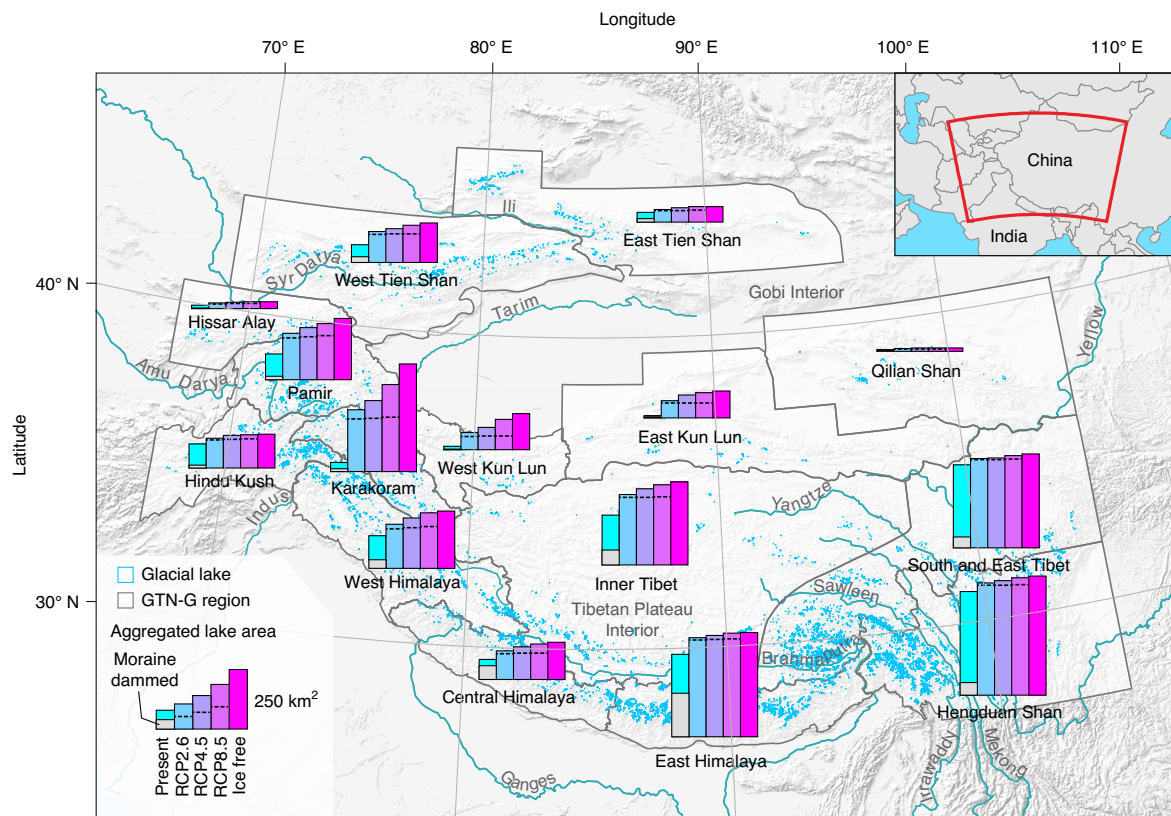


Fig. 1 | Region-wide present and projected glacial lakes to 2050, 2100 and on an ice-free Third Pole. Map showing the geographical extent of the Third Pole and the spatial distribution of its present glacial lakes. Bar charts in different colours denote the present and potential future glacial lake areas (present plus projected results under three RCPs, and under the ice-free scenario) that were aggregated into the Global Terrestrial Network for Glaciers (GTN-G) regions⁴⁶, respectively. The proportional area of present moraine-dammed glacial lakes to all present glacial lakes is shown in grey. Dashed lines show estimated changes in 2050.

Shan mountains and ranges of inner and southeast Tibet as well as the Tien Shan mountains. The Hengduan Shan holds the largest number of glacial lakes (6,571; $436.2 \pm 0.5 \text{ km}^2$), whereas the eastern Himalaya has the most moraine-dammed glacial lakes (1,533; $183.7 \pm 0.4 \text{ km}^2$). At the basin scale, glacial lakes are most abundant in the Brahmaputra River Basin (9,665; $778.8 \pm 0.8 \text{ km}^2$), followed by the Indus, Yangtze, Ganges, Amu Darya and Salween river basins (all with $>1,000$ lakes, Supplementary Fig. 3 and Supplementary Table 2). The Brahmaputra River Basin is also home to the largest number of moraine-dammed glacial lakes (2,331; $212.0 \pm 0.4 \text{ km}^2$).

Glacial lakes on the Third Pole have undergone a notable increase in total area and number since the 1990s^{5–7}. Our analyses show an overall increase of $6.8 \pm 0.1\%$ in glacial lake area and 5.9% in lake number across the Third Pole between 1990 and 2015 (Supplementary Fig. 4 and Supplementary Table 1). We propose that this recent increase has principally been driven by an expansion of moraine-dammed glacial lakes that characterize many of the long, flat, debris-covered glacier tongues in the region. To test this hypothesis, we split the glacial lakes into two categories: moraine-dammed and other-dammed glacial lakes (Methods). We find that if only the moraine-dammed glacial lakes are considered, the area gain is substantially larger at $31.3 \pm 0.3\%$, with an increase in number of 26.7%. In contrast, the size of other-dammed glacial lakes remains virtually unchanged ($-0.02 \pm 0.2\%$), with a slight decrease in number of -1.4%. Still, changes show clear heterogeneity both at regional and basin scales (Supplementary Figs. 4 and 5).

Historical GLOF activity

As GLOF events across the Third Pole have been heavily reported in previous studies^{18–20,29}, we systematically collected and collated these records to better understand their spatial distributions and the characteristics of different source lakes, which were categorized into moraine, ice, bedrock and complex ones depending on the dam type (Fig. 2a; see Supplementary Table 3 for all records assembled). On the basis of this dataset, we found that at least 296 GLOF events from 109 glacial lakes occurred over the Third Pole since 1560 CE. GLOFs in the eastern Himalaya are primarily from the failures of moraine-dammed glacial lakes (Fig. 2c and Supplementary Table 3) and account for ~45% of the past GLOF sources alone. GLOFs resulting from ice-dammed glacial lakes are all reported in the Pamir–Karakoram regions (Fig. 2a), where the prevalent glacier surges have led to repetitive blockage and eventual release of glacial lakes¹⁹. Although most past GLOF sources were related to moraine-dammed glacial lakes (74 out of 109, Fig. 2b), ice- or complex-dammed flood sources (34 out of 109, Fig. 2b) contributed to more than half of the past outbursts (187 out of 296, Fig. 2b) due to the repetitive and high-frequency nature of these events. This is exemplified in the case of Kyagar Tsho (see Fig. 2a for its location and Supplementary Table 3), situated in the headwaters of Yarkant River, which produced at least 33 outburst floods in the past century with an accelerating trend during recent decades³². Practical experience has proven that real-time monitoring and early warning systems are effective in forecasting such active and high-frequency floods resulting from ice dam breaches^{32,33}. The complex-dammed

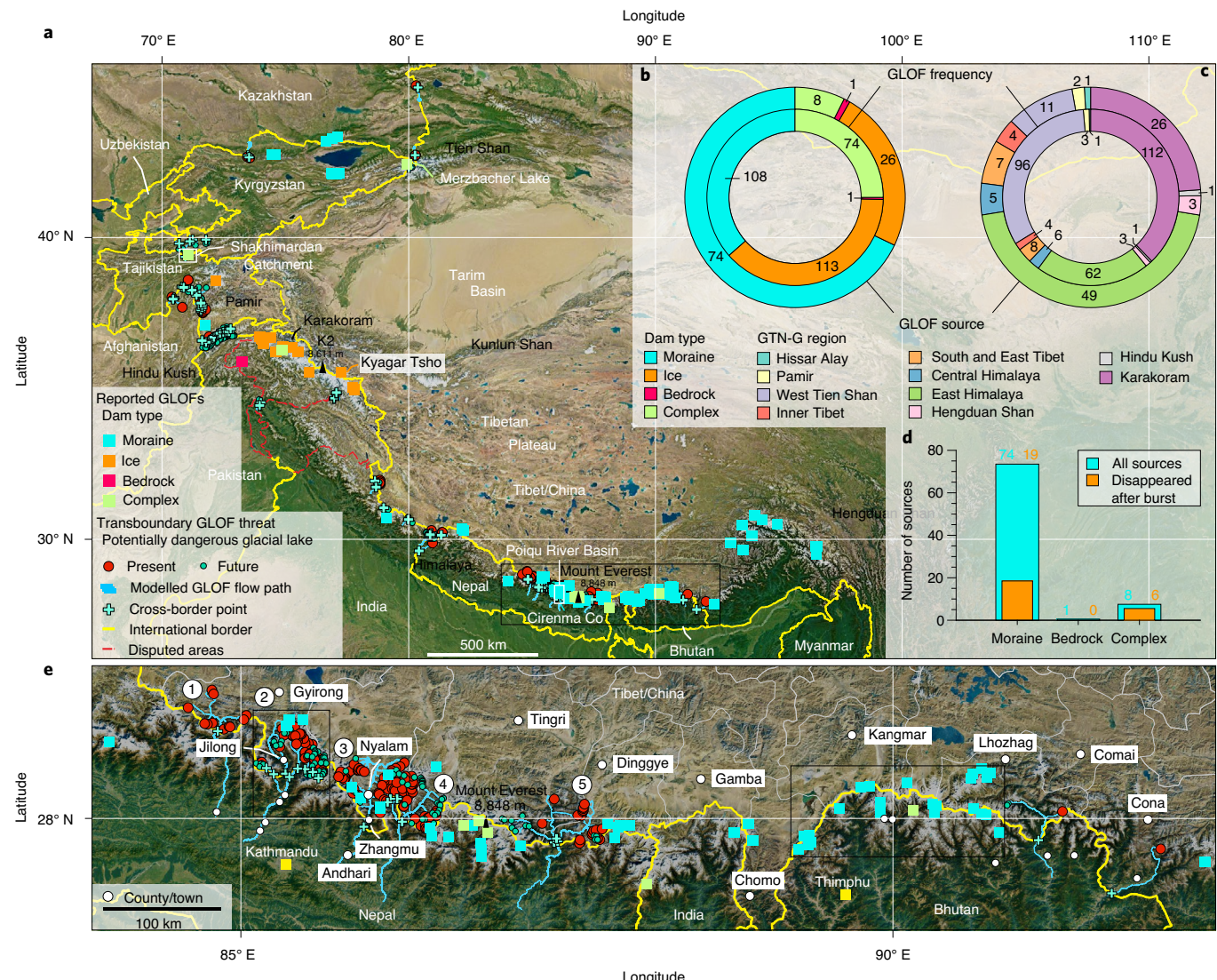


Fig. 2 | Reported historical GLOFs and potential transboundary threats on the Third Pole. **a**, Map showing the spatial distribution of recorded GLOF sources by lake dam type as well as present and projected (ice-free scenario) glacial lakes with possible transboundary GLOF threats across the Third Pole. For ice-dammed GLOF sources, only those with known geographic coordinates are shown (see Supplementary Table 3 for complete records). The black box near the bottom of the panel is the location of **e**. **b**, Double doughnut chart representing the number of past GLOF sources and flood frequency by lake dam type. **c**, Double doughnut chart showing the number of past GLOF sources and flood frequency per region. **d**, Statistics of GLOF sources by lake dam type. Ice-dammed cases were not counted owing to their repetitive nature. **e**, Amplified map showing a hotspot of potential transboundary GLOF threat between China and Nepal, and a historical GLOF hotspot in the eastern Himalaya. The circled numbers represent five concentrated regions with potential transboundary GLOF threats. The capital cities of Nepal and Bhutan are indicated with yellow squares. The left black box is the location of Supplementary Fig. 13 and the right black box is the location of Supplementary Fig. 14. Base maps: Google, Europa Technologies.

glacial lakes are usually positioned on the surface of debris-covered glaciers and are held back by a mix of ice and moraine. These lakes often vanish fully after an outburst (Fig. 2d), but some exceptions exist. For instance, Merzbacher Lake (see Fig. 2a for the specific site and Supplementary Table 3), located upstream of Aksu River, has produced at least 66 recorded outbursts over the last century because of its peculiar geographic situation and water supply modes^{14,34}. The occurrence of floods from such lakes is sudden and difficult to monitor and mitigate, as drainage can occur within or underneath the glacier³⁴.

Present hotspots of GLOF hazard and risk

Based on a conceptual model of GLOF hazard and risk optimized for large-scale automated application (Methods), we implemented

the first quantitative assessment of potential GLOF hazard and risk for a total of 6,958 existing moraine-dammed glacial lakes across the Third Pole and provide hierarchical classifications. This study complements numerous national- to regional-scale GLOF hazard and risk inventories that have previously been undertaken (Supplementary Table 4), allowing a comparison of GLOF hazard and risk across the entire Third Pole. The model considers GLOF hazard on the basis of well-established conditioning and triggering factors³⁰ and identifies infrastructure and communities at risk within downstream simulated flood paths. In contrast to previous work, we evaluate model reliability by validating classification results against those glacial lakes that have generated outburst floods in the past. The model successfully classified GLOF hazard as high or very high for 46 out of the 48 existing glacial lakes (that is,

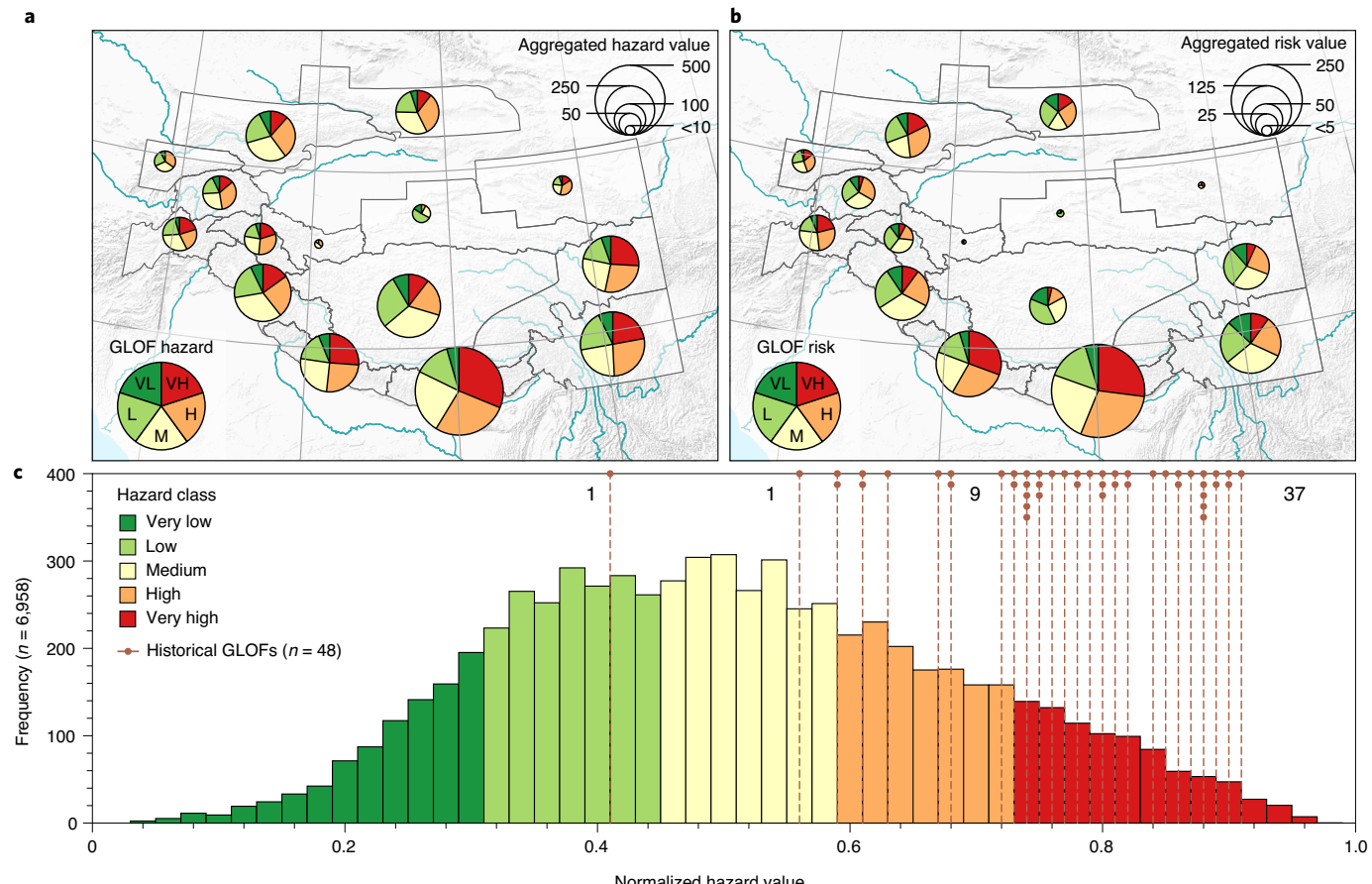


Fig. 3 | Region-wide present GLOF hazard and risk across the Third Pole. **a,b**, Pie charts showing the proportion of different GLOF hazard (**a**) and risk (**b**) levels per region. VL, very low; L, low; M, medium; H, high; VH, very high. Aggregated hazard and risk values are the total sums of normalized values within each region. **c**, Histogram presenting the distribution of GLOF hazard levels across all moraine-dammed glacial lakes assessed. The vertical dashed lines indicate the distribution of assessed GLOF hazard values for glacial lakes where historical GLOFs have been recorded, which were further used to validate the overall model performance. The dots refer to the number of GLOF sources for a given hazard value.

95.8% accuracy, Fig. 3c and Supplementary Table 6), from which the past GLOFs originated. For example, Jialong Co and Cirenma Co, located in eastern Himalaya, have been the origin of several GLOFs since 1960, and are both ranked within the 99th percentile of the most hazardous lakes. Overall, our assessment indicates that one-third (2,323) of all glacial lakes assessed have high to very high hazard levels, and one in six (1,203) glacial lakes would pose a potentially high to very high risk to downstream communities. More than one-third (2,619) of glacial lakes assessed appear not to be dangerous as no downstream infrastructures are evident within the flood paths (see Supplementary Table 5 for all infrastructures considered). On a regional scale, the eastern Himalaya has the highest value in terms of GLOF hazard, which is twice that of the adjacent Hengduan Shan, inner Tibet, central and western Himalaya, and southeast Tibet; three to four times that of the Tien Shan areas; and seven to eight times that of the Pamir, Hindu Kush and Karakoram (Fig. 3a). For GLOF risk, the eastern Himalaya likewise has the highest value, being two to three times that of the central Himalaya, Hengduan Shan and western Himalaya; four times that of southeast Tibet and western Tien Shan; and six to eight times that of inner Tibet, Hindu Kush, eastern Tien Shan and Pamir (Fig. 3b). Notably, some regions such as inner and southeast Tibet present high levels of GLOF hazard (Fig. 3a), but lower levels of GLOF risk (Fig. 3b) owing to much lower exposure values compared with the central and eastern Himalaya (Supplementary Fig. 6). While

mapping of roads and other exposed elements over inner and southeast Tibet is considered less complete than elsewhere³⁵, these results correspond well with other approaches based on gridded data including population density and cropland area that have likewise identified highest risk levels in central and eastern Himalaya³⁶. At the basin scale, the Brahmaputra River Basin has the highest level in terms of GLOF hazard, followed by Ganges, Indus, Salween, Ili, Amu Darya river basins and Tibetan Plateau interior (Supplementary Fig. 7a). However, with respect to GLOF risk, the Ganges River Basin has the highest level, followed by Brahmaputra, Indus, Amu Darya, Ili, Salween and Syr Darya river basins (Supplementary Fig. 7b).

Anticipation of future changes

We expand our assessment to consider how and where GLOF hazard and risk will evolve under continued global warming and glacier shrinking. Future glacial lake formation and associated hazard and risk are considered under three different CO₂ emission scenarios (Representative Concentration Pathways, RCP2.6, RCP4.5 and RCP8.5)³⁷ and projections of a glacier model³⁸ for the middle (2050) and end (2100) of the twenty-first century (Methods). These results are compared with an ice-free scenario which assumes that the Third Pole's glaciers have totally vanished. Our modelling suggests that >13,000 new glacial lakes with a combined maximum area of ~1,510 km² and a combined maximum volume of ~50 km³ could potentially emerge in an ice-free environment (Supplementary

Table 1). This includes the expansion of existing glacial lakes to reach their topographically constrained extent, and potential new glacial lakes forming in depressions within the former bed of glaciers. In total, ~47% of this additional lake area would have already emerged by 2050, and 86% by 2100 under RCP8.5 (or 44% and 56%, respectively, under RCP2.6) (Supplementary Table 1). This future glacial lake development is mostly clustered along the Pamir–Karakoram–Kunlun Shan–Himalaya ranges as well as the western Tien Shan mountains (Fig. 1 and Supplementary Table 1), where the existing glaciers contribute ~74% of the total Third Pole glacier area (Supplementary Table 1). There is notable regional variation in projected glacial lake development from east to west, with regions such as southeast Tibet and eastern Himalaya already revealing close to their maximum lake area by 2050, under all RCP scenarios (Fig. 1). In contrast, in Karakoram, Pamir and western Himalaya, lake area will continue to increase strikingly into the late twenty-first century and beyond. On a basin scale, the future glacial lakes will be expected chiefly at the headwaters of the Indus and Tarim river basins, followed by Amu Darya, Ganges, Brahmaputra river basins and the interior ranges of the Tibetan Plateau (~89% of all projected glacial lakes, Supplementary Fig. 3 and Supplementary Table 2). The Brahmaputra, Ganges and Yangtze river basins almost approach their maximum lake area in 2050 under the three CO₂ emission scenarios, whereas lakes in the Indus and Tarim river basins as well as the Tibetan Plateau interior will continue to expand beyond 2100.

To assess the possible implications of this future glacial lake development on GLOF hazard and risk, we applied the same model as was used for the present glacial lakes, with some slight modifications to account for future unknowns (Methods). For the whole Third Pole region, results indicate that future GLOF hazard and risk will increase by almost threefold relative to current conditions, with obvious regional variations (Fig. 4 and Supplementary Fig. 8). This is considered a conservative maximum estimate given that glacial lakes will appear gradually, and an unknown quantity of moraine dams could breach, and lakes thereby drain, before other lakes have emerged. Nonetheless, under the high-emission scenario RCP8.5, much of the Third Pole could already be approaching a state of ‘peak risk’ by the end of the twenty-first century, or even mid-century in some regions, with risk levels comparable to even the ice-free scenario (Fig. 4). In an ice-free environment, average glacial lake volumes will be ~80% larger than today, while topographic potential for ice/rock avalanche triggering will increase by ~230%, as lakes will be positioned closer to steep mountain headwalls (Supplementary Fig. 9). This suggests that the increase in potential GLOF frequency will generally be more important than the future change in magnitude. Meanwhile, in terms of risk, although overall exposure levels will increase due to the larger number of lakes, future lakes will on average have lower exposure levels (~40% compared with today) as they are located higher, and farther away from existing communities. As a consequence, average risk values per lake will be 14% lower in the future, while the overall number of lakes classified to have high or very high risk levels will increase from 1,203 to 2,963 lakes (that is, by a factor of 2.5). This analysis does not consider future changes in the distribution of population and infrastructure, particularly hydropower, that is expanding higher into alpine valleys³⁹. Likewise, tourism expansion into remote mountain valleys could further enhance risks, while outmigration from rural areas could reduce risk in some cases^{40,41}. Collectively, the Karakoram, Pamir and western Himalaya will be the regions with the most substantial increase in GLOF hazard, while in terms of risk, the largest increases will be in central Himalaya, Karakoram and western Himalaya (Fig. 4 and Supplementary Fig. 8). The eastern Himalaya will remain the primary GLOF hotspot under all assessed future scenarios, while the emergence of the Karakoram as an additional major hotspot of GLOF hazard and risk is most notable over longer timescales under RCP4.5 and RCP8.5, and under the ice-free

scenario. While lake volumes will on average be larger than today, it is clear that even in the future, it is not necessarily the largest lakes that will be the biggest threat to communities (Supplementary Fig. 10). At the basin scale, the future increase in GLOF risk will be greatest in the Indus, Ganges and Amu Darya river basins, with the Ganges River Basin maintaining the highest risk levels under all future scenarios (Supplementary Figs. 11 and 12). By 2100, the Indus River Basin will exhibit the highest GLOF hazard levels (currently exhibited by the Brahmaputra River Basin), with close to a fourfold increase from today under the RCP4.5 scenario.

Potential transboundary threats

The mountain ranges of the Tibetan Plateau and surrounding areas span 11 nations (Fig. 2a), giving rise to potential transboundary natural disasters, especially GLOFs. In fact, several relevant cases have been reported, for instance, in the transboundary Poiqu River Basin between China and Nepal⁴² and the Shakhimardan catchment between Kyrgyzstan and Uzbekistan⁴² (Fig. 2a). A well-known outburst from Cirenma Co (Fig. 2a) in 1981 caused serious devastation, including but not limited to the destruction of the Sino–Nepal Friendship bridge and part of the Nepal Sun Koshi hydropower station, and the loss of 200 lives in Nepal⁴³. Recognizing the broader transboundary threat across the Third Pole, we identified where simulated flood flow paths from existing moraine-dammed glacial lakes intersected with national borders. Consequently, a total of 438 glacial lakes were found to have the potential to produce a transboundary flood, of which 191 were classified to be in the high or very high risk classes (Fig. 2a). Further analysis revealed that ~86% of these potentially dangerous lakes are located between China and Nepal, forming five hotspots of transboundary floods (Fig. 2e). It can be inferred from the illustrated example of one of these hotspots shown in Supplementary Fig. 13 that a possible outburst will have serious effects on downstream transboundary settlements and infrastructures.

The transboundary GLOF threat will amplify in the future. Analysis suggests that the number of future potential transboundary flood sources under the ice-free scenario will roughly double (an additional 464 lakes), with 211 of these lakes classified in the high or very high risk classes (Fig. 2a). The border region between China and Nepal will remain a major hotspot (~42% of all these future dangerous glacial lakes), while the border region between Tajikistan and Afghanistan emerges clearly as an additional potential transboundary hotspot (~36%, up from ~5% at present).

Summary and implications

We conclude that while the most dangerous hotspots of GLOF hazard and risk are now located within the eastern Himalaya, consistent with previous studies^{21,23,36,44} and recorded GLOF events (Supplementary Fig. 10; see Supplementary Fig. 14 for a visual example in the eastern Himalaya), over the course of the twenty-first century, additional hotspots will emerge in the regions to the west, particularly under high-emission scenarios. For Karakoram and Pamir, where glaciers have recently exhibited a stable or slightly positive mass balance⁴⁵, repetitive, high-frequency outburst events associated with ice-dammed glacial lakes will probably remain the dominant GLOF threat for several decades to come. However, the eventual depletion of glaciers in these regions projected during the twenty-first century will see conditions becoming less conducive for glacier surging and ice-dam formation¹⁹, and the threat of moraine- or bedrock-dammed glacial lakes substantially increasing. It is also important to emphasize that climate and related glacial changes as assessed here are just one driver of future GLOF risk; in some regions, future changes in exposure and societal vulnerability could potentially lead to different risk scenarios, especially where political, economic and social conditions facilitate or impede effective disaster risk reduction. Ultimately, determining exactly which lakes are the highest priority for response actions should be guided by consensus across multiple lines of evidence,

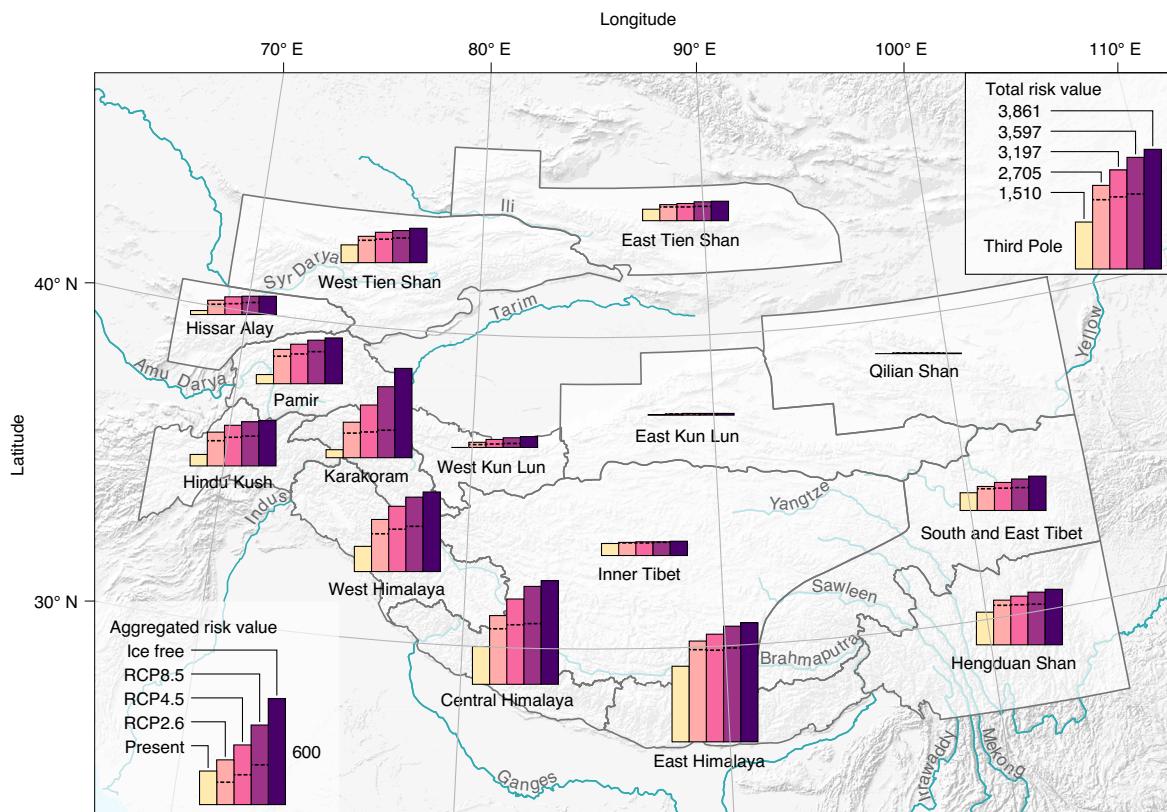


Fig. 4 | Region-wide future changes in GLOF risk to 2050, 2100 and on an ice-free Third Pole. Bar plots indicate projected changes in GLOF risk per region from the present to 2050 and 2100 (under three RCPs) as well as under the ice-free scenario. Dashed lines show estimated changes to 2050. The future GLOF risk was estimated based on currently known infrastructures that are exposed to modelled flood flow paths from potential future lakes and includes the assessed risk from present moraine-dammed glacial lakes (that is, these lakes are assumed to remain in the future). Inset: changes in GLOF risk over the whole Third Pole; note that the scale differs from the regional risk values.

considering not only the wealth of information on existing GLOF hazard and risk (Supplementary Table 4), but also future emerging threats. Particularly where existing and emerging transboundary risks have been identified, risk reduction strategies will require high levels of international planning and cooperation. These transboundary regions represent vital economic corridors of activity, but some suffer from political tensions and challenges that can negatively affect timely data sharing, communication and coordination of early warning and disaster preparedness. We appeal to the relevant nations and international research communities to work together to prevent and mitigate the damages and losses that GLOFs bring to the Third Pole region, and to remain flexible and alert to the new challenges that could emerge under a future warmer climate.

Online content

Any methods, additional references, Nature Research reporting summaries, source data, extended data, supplementary information, acknowledgements, peer review information; details of author contributions and competing interests; and statements of data and code availability are available at <https://doi.org/10.1038/s41558-021-01028-3>.

Received: 2 June 2020; Accepted: 16 March 2021;

Published online: 6 May 2021

References

- Yao, T. et al. Different glacier status with atmospheric circulations in Tibetan Plateau and surroundings. *Nat. Clim. Change* **2**, 663–667 (2012).
- Bolch, T. et al. The state and fate of Himalayan glaciers. *Science* **336**, 310–314 (2012).
- Sorg, A., Bolch, T., Stoffel, M., Solomina, O. & Beniston, M. Climate change impacts on glaciers and runoff in Tien Shan (Central Asia). *Nat. Clim. Change* **2**, 725–731 (2012).
- Hock, R. et al. in *IPCC Special Report on the Ocean and Cryosphere in a Changing Climate* (eds Pörtner H.-O. et al.) Ch. 2 (IPCC, 2019).
- Zhang, G., Yao, T., Xie, H., Wang, W. & Yang, W. An inventory of glacial lakes in the Third Pole region and their changes in response to global warming. *Glob. Planet. Change* **131**, 148–157 (2015).
- Nie, Y. et al. A regional-scale assessment of Himalayan glacial lake changes using satellite observations from 1990 to 2015. *Remote Sens. Environ.* **189**, 1–13 (2017).
- Shugar, D. H. et al. Rapid worldwide growth of glacial lakes since 1990. *Nat. Clim. Change* **10**, 939–945 (2020).
- Linsbauer, A. et al. Modelling glacier-bed overdeepenings and possible future lakes for the glaciers in the Himalaya–Karakoram region. *Ann. Glaciol.* **57**, 119–130 (2016).
- Haeberli, W. et al. New lakes in deglaciating high-mountain regions — opportunities and risks. *Climatic Change* **139**, 201–214 (2016).
- Farinotti, D., Round, V., Huss, M., Compagni, L. & Zekollari, H. Large hydropower and water-storage potential in future glacier-free basins. *Nature* **575**, 341–344 (2019).
- Begam, S., Sen, D. & Dey, S. Moraine dam breach and glacial lake outburst flood generation by physical and numerical models. *J. Hydrol.* **563**, 694–710 (2018).
- Cook, K. L., Andermann, C., Gimbert, F., Adhikari, B. R. & Hovius, N. Glacial lake outburst floods as drivers of fluvial erosion in the Himalaya. *Science* **362**, 53–57 (2018).
- Dubey, S. & Goyal, M. K. Glacial lake outburst flood hazard, downstream impact, and risk over the Indian Himalayas. *Water Resour. Res.* **56**, e2019WR026533 (2020).

14. Carrivick, J. L. & Tweed, F. S. A global assessment of the societal impacts of glacier outburst floods. *Glob. Planet. Change* **144**, 1–16 (2016).
15. Emmer, A. GLOFs in the WOS: bibliometrics, geographies and global trends of research on glacial lake outburst floods (Web of Science, 1979–2016). *Nat. Hazards Earth Syst. Sci.* **18**, 813–827 (2018).
16. Yang, K. et al. Recent climate changes over the Tibetan Plateau and their impacts on energy and water cycle: a review. *Glob. Planet. Change* **112**, 79–91 (2014).
17. Harrison, S. et al. Climate change and the global pattern of moraine-dammed glacial lake outburst floods. *Cryosphere* **12**, 1195–1209 (2018).
18. Hewitt, K. & Liu, J. Ice-dammed lakes and outburst floods, Karakoram Himalaya: historical perspectives on emerging threats. *Phys. Geogr.* **31**, 528–551 (2010).
19. Bhambri, R. et al. Ice-dams, outburst floods, and movement heterogeneity of glaciers, Karakoram. *Glob. Planet. Change* **180**, 100–116 (2019).
20. Nie, Y. et al. An inventory of historical glacial lake outburst floods in the Himalayas based on remote sensing observations and geomorphological analysis. *Geomorphology* **308**, 91–106 (2018).
21. Allen, S. K., Zhang, G., Wang, W., Yao, T. & Bolch, T. Potentially dangerous glacial lakes across the Tibetan Plateau revealed using a large-scale automated assessment approach. *Sci. Bull.* **64**, 435–445 (2019).
22. Khanal, N. R. et al. A comprehensive approach and methods for glacial lake outburst flood risk assessment, with examples from Nepal and the transboundary area. *Int. J. Water Resour. Dev.* **31**, 219–237 (2015).
23. Veh, G., Korup, O. & Walz, A. Hazard from Himalayan glacier lake outburst floods. *Proc. Natl Acad. Sci. USA* **117**, 907–912 (2020).
24. Fujita, K. et al. Potential flood volume of Himalayan glacial lakes. *Nat. Hazards Earth Syst. Sci.* **13**, 1827–1839 (2013).
25. Neupane, R., Chen, H. & Cao, C. Review of moraine dam failure mechanism. *Geomat. Nat. Hazards Risk* **10**, 1948–1966 (2019).
26. Allen, S. K., Rastner, P., Arora, M., Huggel, C. & Stoffel, M. Lake outburst and debris flow disaster at Kedarnath, June 2013: hydrometeorological triggering and topographic predisposition. *Landslides* **13**, 1479–1491 (2016).
27. Zaginayev, V. et al. Reconstruction of glacial lake outburst floods in northern Tien Shan: implications for hazard assessment. *Geomorphology* **269**, 75–84 (2016).
28. Emmer, A. & Cochachin, A. The causes and mechanisms of moraine-dammed lake failures in the Cordillera Blanca, North American Cordillera, and Himalayas. *AUC Geographica* **48**, 5–15 (2013).
29. Veh, G., Korup, O., von Specht, S., Roessner, S. & Walz, A. Unchanged frequency of moraine-dammed glacial lake outburst floods in the Himalaya. *Nat. Clim. Change* **9**, 379–383 (2019).
30. GAPHAZ Assessment of Glacier and Permafrost Hazards in Mountain Regions – Technical Guidance Document (Standing Group on Glacier and Permafrost Hazards in Mountains (GAPHAZ) of the International Association of Cryospheric Sciences (IACS) and the International Permafrost Association (IPA), 2017).
31. Haeberli, W., Schaub, Y. & Huggel, C. Increasing risks related to landslides from degrading permafrost into new lakes in de-glaciating mountain ranges. *Geomorphology* **293**, 405–417 (2017).
32. Yin, B., Zeng, J., Zhang, Y., Huai, B. & Wang, Y. Recent Kyagar glacier lake outburst flood frequency in Chinese Karakoram unprecedented over the last two centuries. *Nat. Hazards* **95**, 877–881 (2019).
33. Haemmig, C. et al. Hazard assessment of glacial lake outburst floods from Kyagar glacier, Karakoram Mountains, China. *Ann. Glaciol.* **55**, 34–44 (2014).
34. Shangguan, D. et al. Quick release of internal water storage in a glacier leads to underestimation of the hazard potential of glacial lake outburst floods from Lake Merzbacher in Central Tian Shan Mountains. *Geophys. Res. Lett.* **44**, 9786–9795 (2017).
35. Barrington-Leigh, C. & Millard-Ball, A. The world's user-generated road map is more than 80% complete. *PLoS ONE* **12**, e0180698 (2017).
36. Wang, S., Qin, D. & Xiao, C. Moraine-dammed lake distribution and outburst flood risk in the Chinese Himalaya. *J. Glaciol.* **61**, 115–126 (2015).
37. Meinshausen, M. et al. The RCP greenhouse gas concentrations and their extensions from 1765 to 2300. *Climatic Change* **109**, 213 (2011).
38. Huss, M. & Hock, R. Global-scale hydrological response to future glacier mass loss. *Nat. Clim. Change* **8**, 135–140 (2018).
39. Schwanghart, W., Worni, R., Huggel, C., Stoffel, M. & Korup, O. Uncertainty in the Himalayan energy–water nexus: estimating regional exposure to glacial lake outburst floods. *Environ. Res. Lett.* **11**, 074005 (2016).
40. Ziegler, A. D. et al. Pilgrims, progress, and the political economy of disaster preparedness — the example of the 2013 Uttarakhand flood and Kedarnath disaster. *Hydrocl. Process.* **28**, 5985–5990 (2014).
41. von Dach, W. et al. *Safer Lives and Livelihoods in Mountains: Making the Sendai Framework for Disaster Risk Reduction Work for Sustainable Mountain Development* (Centre for Development and Environment (CDE), University of Bern, with Bern Open Publishing (BOP), 2017).
42. Petrakov, D. A. et al. Putting the poorly documented 1998 GLOF disaster in Shakhimardan River valley (Alay range, Kyrgyzstan/Uzbekistan) into perspective. *Sci. Total Environ.* **724**, 138287 (2020).
43. Wang, W. et al. Integrated hazard assessment of Cirenmaco glacial lake in Zhangzangbo Valley, Central Himalayas. *Geomorphology* **306**, 292–305 (2018).
44. Wang, S., Che, Y. & Xinggang, M. Integrated risk assessment of glacier lake outburst flood (GLOF) disaster over the Qinghai–Tibetan Plateau (QTP). *Landslides* **17**, 2849–2863 (2020).
45. Azam, M. F. et al. Review of the status and mass changes of Himalayan–Karakoram glaciers. *J. Glaciol.* **64**, 61–74 (2018).
46. GTN-G Glacier Regions (Global Terrestrial Network for Glaciers, 2017); <https://doi.org/10.5904/gtn-glacreg-2017-07>

Publisher's note Springer Nature remains neutral with regard to jurisdictional claims in published maps and institutional affiliations.

© The Author(s), under exclusive licence to Springer Nature Limited 2021

Methods

Glacial lake delineation and lake changes. We used Landsat satellite imagery to outline the boundaries of glacial lakes that are defined as water bodies formed primarily by glaciation and fed by glacial/snow melts, and are situated on the surface, adjacent or downstream of a glacier, or on palaeoglaciation landforms⁴⁷ across the Third Pole. Two time windows, 1990 ± 4 and 2015 ± 1 , were chosen to reveal the present state of glacial lakes and their changes over the last ~ 25 years. The selection was determined largely by the availability of Landsat datasets in such a large area. To minimize the effects of ice or seasonal snow cover on glacial lake mapping in these high elevations, we picked images mostly from the warm season (June to November), which corresponds roughly to the highest and most stable water areas/levels of the lakes in a hydrological year⁴⁸. Overall, we used a total of 403 Landsat 4–5 Thematic Mapper (TM) scenes (97.8% from the warm season) for the 1990 epoch and 294 Landsat 8 Operational Land Imager (OLI) scenes (100% in the warm season) for the 2015 period (Supplementary Figs. 1 and 2a,b). We also gave priority to images with no or little cloud coverage, that is, an average cloud cover percentage of 7.7% and 4.2% for 1990 and 2015, respectively (Supplementary Figs. 1 and 2c). Landsat images were obtained from the US Geological Survey (USGS) data portal with a spatial resolution of 30 m. Images were first converted from the digital numbers to the top of atmosphere. Landsat 8 OLI images were further fused using a nearest neighbour diffusion-based pan-sharpening algorithm⁴⁹ to improve their spatial resolution to 15 m.

An automated water body classification algorithm⁵⁰ based on global-local threshold segmentation for water indices greyscale images was applied to extract all water bodies from the Landsat images. A slope threshold of $<20^\circ$ as well as a shaded relief threshold of >0.25 were employed to alleviate the disturbances from mountain shadows⁵⁰. Subsequently, careful visual inspection and manual re-editing were carried out to remove other water bodies (for example, reservoirs, rivers and small streams) and to correct the wrongly mapped glacial lakes based on corresponding Landsat scenes, online maps and other glacial lake datasets^{5,47,51–53} available for the Third Pole. A 10 km buffer^{5,52} around the Randolph Glacier Inventory (RGI 6.0)⁵⁴ was used to preliminarily determine the distribution of what could be considered glacial lakes. However, to ensure the integrity and reliability of our inventory, we also included additional glacial lakes in areas where glaciers are missing from the RGI 6.0 dataset⁵⁵. Both the glacial lake datasets for 1990 and 2015 were then cross-checked and attributed. The area of all glacial lakes was calculated based on the universal transverse mercator (UTM) projected coordinate system and their uncertainty (δ) was estimated using the formula⁵⁶: $\delta = P/G \times G^2/2 \times 0.6872$, where P is the perimeter of the glacial lake and G is the spatial resolution of the images used. Lastly, we selected all glacial lakes $\geq 0.01 \text{ km}^2$ and superimposed them in a high-resolution Google Earth 3D view mode together with the corresponding Landsat scenes to distinguish the moraine-dammed glacial lakes separately. The remaining lakes were grouped and termed ‘other-dammed glacial lakes’. Lakes dammed with ice or lying on the surface of glaciers were not included in the temporal change analyses due to their transient character and large seasonal fluctuations.

The relative change in glacial lake area between 1990 and 2015 and its uncertainty were estimated using the following equations:

$$R = \frac{A_2 - A_1}{A_1} \times 100\%$$

$$\delta R = \sqrt{\left(\frac{\delta A}{A_2 - A_1}\right)^2 + \left(\frac{\delta A_1}{A_1}\right)^2} \times R$$

where R is the relative change in glacial lake area and δR is its uncertainty; A_1, A_2 are the lake areas at the beginning and end of the period, respectively; and $\delta A_1, \delta A_2$ are their uncertainties, $\delta A = \sqrt{\delta A_1^2 + \delta A_2^2}$.

Modelling of future glacial lakes. Glacier-bed topography, that is, ice-free digital elevation model (DEM) can be estimated using model approaches that determine local ice thickness based on the characteristics of surface topography and considerations of ice-flow dynamics⁵. The potential sites of future glacial lake formation under scenarios of complete deglaciation can then be projected by detecting overdeepenings on the glacier-bed. Here we used the latest global glacier ice thickness dataset⁴⁷ consisting of a consensus of five different ice thickness models as well as the 30 m Advanced Land Observing Satellite Global Digital Surface Model (ALOS AW3D30 v2.2) to extract the bed topography of all Third Pole glaciers. Three analytical steps were performed to determine the possible sites of future glacial lake formation: (1) glacier areas with slopes $<20^\circ$ were mapped first as potential locations of glacier-bed overdeepenings as lakes normally form in flat topography; (2) depressions in the glacier bed were detected by filling them using a classic filling algorithm⁵⁸, while a slope raster was generated based on the filled glacier-bed topographies; and (3) depressions with a slope $<1^\circ$ were identified⁵ and intersected with the layer of possible overdeepenings obtained in the first step to generate the final layer of the possible future lakes. Ultimately, we selected all modelled overdeepenings $\geq 0.01 \text{ km}^2$ as the potential sites of future lake formation, to ensure comparability to the glacial lake inventories in 1990 and 2015. The area and volume of all modelled future glacial lakes were estimated based on a bathymetry raster that was derived from the difference between the

overdeepenings-filled DEM and the original glacier-bed topography. The mean and maximum depth of each glacial lake was also estimated using the detected depression extent and its bathymetry raster. In general, ice-thickness models have proven robust in detecting the locations of overdeepenings⁵⁹, although local uncertainties in ice-thickness estimates (and thereby volume of the overdeepenings and associated future lake) could be on the order of $\pm 100\%$ for individual cases⁶⁰. Likewise, dam composition (moraine or bedrock) cannot be distinguished for future lakes, and lake volumes will be ultimately determined by dam geometry and the presence of an outlet channel.

To estimate the time horizon in which potential future glacial lakes could emerge, we simulated glacier recession based on an ensemble of 14 global circulation models of the Climate Model Intercomparison Project Phase 5 (ref. ⁶¹) under three different CO₂ emission scenarios — RCP2.6, RCP4.5 and RCP8.5, in addition to the hypothetical end case with a completely ice-free Third Pole. Two major time horizons over the course of the twenty-first century, 2050 and 2100, were considered. The Global Glacier Evolution Model (GloGEM)³⁸ was employed to model the evolution of all individual RGI 6.0 glaciers based on projected climate forcing until 2100. GloGEM resolves all components of the glacier surface mass balance and computes changes in glacier geometry (thickness, length) in annual time steps. Results for the ensemble of global circulation models have been averaged for the three considered RCPs. The minimum elevation for each glacier at both 2050 and 2100 under each RCP scenario was calculated and used to determine the exposed overdeepenings at each time step. We assume that the potential glacial lake is forming or has formed if the modelled minimum elevation of its parent glacier is greater than or equal to the elevation of the modelled overdeepening that was retrieved based on the filled glacier-bed topographies.

GLOF hazard assessment and validation. Moraine-dammed glacial lakes dominate past GLOFs recorded in most of the world¹⁷, especially in the Himalaya^{20,29}, and their evolution can be directly linked to atmospheric warming and glacial recession¹⁷. Hence, for the current GLOF hazard and risk assessment, we focused on such lakes. A conceptual model²¹ was used to assess hazard and risk for 6,958 existing moraine-dammed proglacial lakes across the Third Pole. The model does not apply to some glacial lakes situated on the surface or flanks of debris-covered glaciers, as predisposing and triggering factors in these cases are different. Furthermore, we recognize the transition and complexity that occurs between different lake types, meaning that some degree of subjectivity in lake classification cannot be avoided. The model defines three indices²¹: the GLOF risk index as a function of the hazard index (combining likelihood and potential magnitude of a GLOF) and exposure index (potential for people and infrastructure to be affected). Here we improved the model for large-scale implementation so that it can run on a single glacial lake object iteratively. The large-scale assessment was based on a single UTM grid zone. All calculations and analyses described below were based on the 90 m Multi-Error-Removed Improved-Terrain (MERIT) DEM⁶², which is proven to have the best performance on the Third Pole⁴³.

The potential hazard of a GLOF was defined based on four key factors²¹, which encompass well-established processes that drive GLOF triggering and magnitude³⁰. (1) Lake volume was calculated using a lake depth-area-volume empirical relationship⁶⁴ and used as a proxy for possible maximum flood magnitude. (2) Total watershed area upstream of each glacial lake was used as an indicator of the potential for heavy rain and glacier/snow melt runoff to flow into the lake or cause it to overflow^{20,26}. (3) The likelihood of ice and/or rock avalanches triggering an outburst was calculated based on the concept of topographic potential which includes: the potential for ice and/or rock to detach (parameterized by slope angle); and the potential for the ice and/or rock avalanche to reach a glacial lake (parameterized by the overall trajectory slope or angle of reach). Due to the quality of available glacier datasets at such a large scale, we did not distinguish whether the surrounding slopes were rock or ice-covered. Thus, we assumed that an avalanche was possible from any slope $>30^\circ$, and the resulting avalanche could feasibly impact the lake where the overall slope trajectory is $>14^\circ$ (tangent angle = 0.25)⁶⁵. (4) Downstream slope of the lake dam was considered to be an important factor controlling dam stability and the potential for self-destruction. It is also relevant for the erosional capacity of a GLOF event in downstream areas. This factor was calculated as the average horizontal downstream slope of each lake in three different buffer zones depending on different lake areas (A) intervals ($A \geq 0.1 \text{ km}^2, 900 \text{ m}; 0.1 > A \geq 0.05 \text{ km}^2, 600 \text{ m}; 0.05 > A \geq 0.01 \text{ km}^2, 300 \text{ m}$). These intervals were derived empirically based on careful analyses of a large number of lakes using high-resolution satellite images.

All factors were then normalized to 0 to 1 using the percent ranking method and assumed to have equal weight to the hazard of a GLOF event. For display and comparative purposes, hazards of all glacial lakes were eventually classified into five levels (very low, low, medium, high, very high) using the natural breaks (Jenks) method and then were aggregated to each region and river basin based on the sum of all lake hazard levels.

The verification of model outcomes is highly dependent on empirical information²¹. Here, to verify the results from the GLOF hazard assessment and provide the historical context of GLOF activity, we compiled the most complete inventory of past GLOFs over the Third Pole. Thus, we collected and re-evaluated almost all of the historical GLOF events (Supplementary Table 3) that have been

reported on the Third Pole and found a total of 296 GLOF events from 109 glacial lakes. Finally, 48 moraine-dammed glacial lakes that did not disappear after previous GLOFs and remained $\geq 0.01 \text{ km}^2$ in the 2015 epoch were used to validate the hazard assessment.

GLOF exposure and risk. Exposure represents the presence of people, livestock, infrastructure and other assets that could be threatened by potential GLOF hazard²¹. Here we used infrastructures (such as buildings, highways, railways and historic places, see Supplementary Table 5 for all features used) to characterize the communities and populations that might be affected within a potential GLOF flow path, which was simulated using the GIS-based modified single-flow hydrological model⁶⁶. All infrastructure features were downloaded from OpenStreetMap (accessed 1 August 2019) and were converted to a raster grid. The maximum downstream flow distance for each lake path was determined based on an empirically derived worst-case scenario defined by the angle of reach from the source lake, with a tangent angle = 0.05 (3° angle of reach)⁶⁷. Beyond this flow distance, damages from a GLOF are not expected. The sum of the angle of reach for each OpenStreetMap raster pixel that is exposed to the lake flow path was aggregated as the quantified measure of exposure for each glacial lake. As of 2016, the OpenStreetMap was considered to be 83% globally complete and increasing rapidly, although generally lower (yet relatively homogeneous) levels of completeness are seen over the Third Pole³⁵. The exception is Nepal where intense humanitarian mapping efforts have led to near total completeness.

The exposure values for each glacial lake were also normalized to 0 to 1 using the percent ranking method and then multiplied with the normalized hazard value to give the final risk level associated with each lake. The risk values of all glacial lakes (except those with an exposure value of zero indicating no risk to downstream communities) were divided into five classes using the natural breaks (Jenks) method and aggregated to each region and river basin to obtain their overall risk levels. In the absence of reasonable proxy variables at such a large scale, the vulnerability component of risk was not considered here.

Future GLOF hazard and risk assessments. The same modelling approach was also applied to assess future GLOF hazards and risks for all modelled glacial lakes formed at 2050 and 2100 under three different RCPs and the ice-free scenario. The difference was that the current topography of the glacier areas was substituted by the modelled glacier-bed topography and then the selected factors were calculated for these future scenarios. However, because we cannot judge whether these potential glacial lakes will be dammed by moraine or bedrock, and resulting dam geometries are highly uncertain, we used the average dam slope of present glacial lakes in each region or river basin to characterize all modelled lakes in the same region or basin. Likewise, no robust basis exists to predict the future development of downstream infrastructure and communities across all of the Third Pole; thus, the future risk assessment considers only the change in exposure of existing infrastructures and communities.

Data availability

The Landsat datasets are freely available from the USGS data portal (<https://glovis.usgs.gov/>). The Randolph Glacier Inventory 6.0 (ref. ⁵⁴) data are freely available at <http://www.glims.org/RGI/>. The ALOS Global Digital Surface Model (AW3D30 v2.2) is freely available at <https://www.eorc.jaxa.jp/ALOS/en/aw3d30/index.htm>. The Multi-Error-Removed Improved-Terrain (MERIT) DEM is freely available at http://hydro.iis.u-tokyo.ac.jp/~yamada1/MERIT_DEM/ on reasonable request. The OpenStreetMap data are freely obtained from <http://www.openstreetmap.org/> and available under the Open Database License (<http://www.openstreetmap.org/copyright>). The composite glacier ice thickness data are available at <https://www.research-collection.ethz.ch/handle/20.500.11850/315707>. The produced glacial lake inventories and modelled future lakes as well as relevant assessment results are available at Zenodo under the identifier <https://doi.org/10.5281/zenodo.4477945>.

Code availability

The GLOF hazard and risk assessment models are available at Zenodo under the identifier <https://doi.org/10.5281/zenodo.4477947>. Additional model or code used in this study are available from the corresponding authors on request.

References

47. Maharjan, S. B. et al. *The Status of Glacial Lakes in the Hindu Kush Himalaya*. ICIMOD Research Report 2018/1 (International Centre for Integrated Mountain Development (ICIMOD), 2018).
48. Zhang, Y., Zhang, G. & Zhu, T. Seasonal cycles of lakes on the Tibetan Plateau detected by Sentinel-1 SAR data. *Sci. Total Environ.* **703**, 135563 (2020).
49. Sun, W., Chen, B. & Messinger, D. Nearest-neighbor diffusion-based pan-sharpening algorithm for spectral images. *Opt. Eng.* **53**, 013107 (2014).
50. Zhang, G. et al. Automated water classification in the Tibetan Plateau using Chinese GF-1 WVF data. *Photogramm. Eng. Remote Sens.* **83**, 509–519 (2017).
51. Wang, X. et al. Changes of glaciers and glacial lakes implying corridor-barrier effects and climate change in the Hengduan Shan, southeastern Tibetan Plateau. *J. Glaciol.* **63**, 535–542 (2017).
52. Wang, X. et al. Changes of glacial lakes and implications in Tian Shan, central Asia, based on remote sensing data from 1990 to 2010. *Environ. Res. Lett.* **8**, 044052 (2013).
53. Wang, X., Liu, Q., Liu, S., Wei, J. & Jiang, Z. Heterogeneity of glacial lake expansion and its contrasting signals with climate change in Tarim Basin, Central Asia. *Environ. Earth Sci.* **75**, 696 (2016).
54. RGI Consortium *Randolph Glacier Inventory — A Dataset of Global Glacier Outlines: Version 6.0: Technical Report* (Global Land Ice Measurements from Space (GLIMS), 2017); <https://doi.org/10.7265/N5-RGI-60>
55. Sakai, A. Brief communication: updated GAMDAM glacier inventory over high-mountain Asia. *Cryosphere* **13**, 2043–2049 (2019).
56. Hanshaw, M. N. & Bookhagen, B. Glacial areas, lake areas, and snow lines from 1975 to 2012: status of the Cordillera Vilcanota, including the Quelccaya Ice Cap, northern central Andes, Peru. *Cryosphere* **8**, 359–376 (2014).
57. Farinotti, D. et al. A consensus estimate for the ice thickness distribution of all glaciers on Earth. *Nat. Geosci.* **12**, 168–173 (2019).
58. Planchon, O. & Darboux, F. A fast, simple and versatile algorithm to fill the depressions of digital elevation models. *Catena* **46**, 159–176 (2002).
59. Linsbauer, A., Paul, F. & Haeberli, W. Modeling glacier thickness distribution and bed topography over entire mountain ranges with GlabTop: application of a fast and robust approach. *J. Geophys. Res. Earth Surf.* **117**, F03007 (2012).
60. Farinotti, D. et al. How accurate are estimates of glacier ice thickness? Results from ITMIX, the Ice Thickness Models Intercomparison eXperiment. *Cryosphere* **11**, 949–970 (2017).
61. Taylor, K. E., Stouffer, R. J. & Meehl, G. A. An overview of CMIP5 and the experiment design. *Bull. Am. Meteorol. Soc.* **93**, 485–498 (2012).
62. Yamazaki, D. et al. A high-accuracy map of global terrain elevations. *Geophys. Res. Lett.* **44**, 5844–5853 (2017).
63. Liu, K. et al. Global open-access DEM performances in Earth's most rugged region High Mountain Asia: a multi-level assessment. *Geomorphology* **338**, 16–26 (2019).
64. Huggel, C., Kääb, A., Haeberli, W., Teysseire, P. & Paul, F. Remote sensing based assessment of hazards from glacier lake outbursts: a case study in the Swiss Alps. *Can. Geotech. J.* **39**, 316–330 (2002).
65. Schneider, D., Huggel, C., Haeberli, W. & Kaitna, R. Unraveling driving factors for large rock–ice avalanche mobility. *Earth Surf. Process. Landf.* **36**, 1948–1966 (2011).
66. Huggel, C., Kääb, A., Haeberli, W. & Krummenacher, B. Regional-scale GIS-models for assessment of hazards from glacier lake outbursts: evaluation and application in the Swiss Alps. *Nat. Hazards Earth Syst. Sci.* **3**, 647–662 (2003).
67. Huggel, C., Haeberli, W., Kääb, A., Bieri, D. & Richardson, S. An assessment procedure for glacial hazards in the Swiss Alps. *Can. Geotech. J.* **41**, 1068–1083 (2004).

Acknowledgements

We thank all those who made any data used here freely available. This work was funded by the Strategic Priority Research Program of the Chinese Academy of Sciences (XDA20030101) and the National Key Research and Development Program of China (2017YFB0504204). The contribution of S.K.A. and G.Q.Z. was partially supported by the Swiss National Science Foundation (IZLCZ2_169979/1), and counterpart grant from the National Natural Science Foundation of China (21661132003). A special acknowledgement goes to the China–Pakistan Joint Research Center on Earth Sciences that supported the implementation of this work.

Author contributions

Conceptualization: G.Z., S.K.A., A.B., M.S. Data preparation and model calculations: G.Z., A.B., M.H., G.Q.Z., J.L., Y.Y., T.Y., W.C. Funding acquisition: A.B., S.K.A., G.Q.Z. Methodology: G.Z., S.K.A., M.H. Visualization: G.Z. Project administration: A.B., M.S. Writing, original draft: G.Z., S.K.A., J.B.-C., M.S. Writing, review, and editing: all authors.

Competing interests

The authors declare no competing interests.

Additional information

Supplementary information The online version contains supplementary material available at <https://doi.org/10.1038/s41558-021-01028-3>.

Correspondence and requests for materials should be addressed to A.B. or M.S.

Peer review information *Nature Climate Change* thanks Rakesh Bhambri, Adam Emmer and Kristyna Falatkova for their contribution to the peer review of this work.

Reprints and permissions information is available at www.nature.com/reprints.